

# ***Irradiation of Miniature Fuel Specimens in the High Flux Isotope Reactor***

**Nuclear Technology  
Research and Development**

Approved for public release.  
Distribution is unlimited.

***Prepared for  
U.S. Department of Energy  
Advanced Fuels Campaign  
C.M. Petrie, J.R. Burns, R.N. Morris, K.R.  
Smith, A.G. Le Coq, K.A. Terrani  
Oak Ridge National Laboratory  
June 28, 2018  
NTRD: M2NT-18OR020203041***





#### **DISCLAIMER**

This information was prepared as an account of work sponsored by an agency of the U.S. Government. Neither the U.S. Government nor any agency thereof, nor any of their employees, makes any warranty, expressed or implied, or assumes any legal liability or responsibility for the accuracy, completeness, or usefulness, of any information, apparatus, product, or process disclosed, or represents that its use would not infringe privately owned rights. References herein to any specific commercial product, process, or service by trade name, trade mark, manufacturer, or otherwise, does not necessarily constitute or imply its endorsement, recommendation, or favoring by the U.S. Government or any agency thereof. The views and opinions of authors expressed herein do not necessarily state or reflect those of the U.S. Government or any agency thereof.



## **SUMMARY**

The Advanced Fuels Campaign (AFC) within the US Department of Energy (DOE) Office of Nuclear Energy is considering several advanced ceramic fuels for use in light water reactors (LWRs) and/or advanced reactor concepts. Advanced fuels, such as uranium carbide (UC), uranium nitride (UN), and uranium silicide ( $\text{U}_3\text{Si}_2$ ) offer increased uranium density and enhanced thermophysical properties compared to conventional  $\text{UO}_2$  fuel, while maintaining an acceptably high melting point. Enhancements to traditional  $\text{UO}_2$  are also being considered that would increase the thermal conductivity of the fuel and fission product retention through various additives. However, some of these advanced fuels have very limited information available on their irradiation performance (microstructural evolution, swelling, fission gas release, etc.), particularly for the range of temperature and burnup that are relevant for LWR fuel pins. To address this issue, Oak Ridge National Laboratory has developed an experimental facility to irradiate miniature fuel specimens in the High Flux Isotope Reactor (HFIR). The small size of the fuel specimens simplifies the design, analysis, and post-irradiation evaluations. Post-irradiation examination will provide basic data on the stability and behavior of advanced fuels as a function of temperature and burnup. This report briefly summarizes the experiment facility design concept and the assembly of the first set of experiments. The experiment contains six different types of UN-based fuel kernels UN TRISO particles with varying densities, impurity levels, and burnable absorber contents. The experiments were successfully assembled, welded, evaluated, and delivered to the HFIR along with a complete quality assurance fabrication package. Pictures of the assembly process are included in this report. The experiment is planned for insertion into the HFIR during cycle 480 (June 2018).



## CONTENTS

SUMMARY .....	iii
ACRONYMS .....	ix
ACKNOWLEDGMENTS .....	x
1. OBJECTIVE.....	1
2. INTRODUCTION.....	1
3. EXPERIMENT ANALYSIS METHODOLOGY .....	2
3.1 Experiment design concept .....	2
3.2 Neutronics analysis .....	3
3.3 Thermal analysis .....	4
3.4 Initial Test Matrix .....	5
4. EXPERIMENT ANALYSIS RESULTS.....	6
4.1 Neutronics analysis results.....	6
4.2 Thermal analysis results.....	9
5. EXPERIMENT FABRICATION .....	12
5.1 Sub-capsules Assembly.....	12
5.2 Target Assembly .....	14
5.3 Basket Assembly.....	15
5.4 Fabrication Package and Delivery to HFIR .....	16
6. SUMMARY AND CONCLUSIONS .....	17
7. REFERENCES .....	17
APPENDIX A. FABRICATION AND QUALITY ASSURANCE DOCUMENTATION FOR EXPERIMENTS.....	A-1

## FIGURES

Figure 1. Irradiation design concept. ....	3
Figure 2. 3-D solid model for a single irradiation target and the resulting finite element mesh with $\frac{1}{4}$ -symmetry. ....	4
Figure 3. Polished cross-sectional image of UN TRISO particle ( <i>left</i> ) and image of UN kernels ( <i>right</i> ). ....	5
Figure 4. Heat generation rate (HGR) in titanium components vs. axial distance from the core midplane (z) at beginning of cycle (BOC) and end of cycle (EOC). Exponential fits to the calculated data are shown with goodness of fit parameter $R^2$ . ....	7
Figure 5. Heat generation rate (HGR) in the molybdenum tubes vs. axial distance from the core midplane (z) at beginning of cycle (BOC) and end of cycle (EOC). Exponential fits to the calculated data are shown with goodness of fit parameter $R^2$ . ....	7
Figure 6. Calculated fuel fission rate (solid lines) and burnup (dashed lines) vs. number of HFIR cycles for three different enrichment levels. Results are for fuel located at the core midplane in radial targets oriented toward the HFIR core. ....	9
Figure 7. EOC temperature contours (in °C) with peak fuel heating rates for a target loaded in an inner radial position with six UN sub-capsules. Results show all target components ( <i>top</i> ), a single center sub-assembly ( <i>middle</i> ), the fuel kernels from the center sub-assembly ( <i>bottom left</i> ), and the temperature monitor from the center sub-assembly ( <i>bottom right</i> ). ....	10
Figure 8. Design gas gaps between the sub-capsules and the target housing vs. axial distance from the core midplane for inner radial target positions and outer radial target positions. ....	11
Figure 9. Fuel temperature vs. distance from the core midplane (z) for an inner radial target position at beginning of cycle (BOC) and end of cycle (EOC). Error bars indicate the extreme fuel temperatures at each location. ....	11
Figure 10. Fuel temperature vs. distance from the core midplane (z) for an outer radial target position at beginning of cycle (BOC) and end of cycle (EOC). Error bars indicate the extreme fuel temperatures at each location. ....	12
Figure 11. Sub-capsule part layout ( <i>top</i> ), kernel fuel inside a cup ( <i>bottom left</i> ), and TRISO particle fuel inside a different cup ( <i>bottom right</i> ). ....	13
Figure 12. Top view of a loaded sub-capsule without its end cap ( <i>left</i> ) and welded sub-capsules ( <i>right</i> ). ....	14
Figure 13. Parts layout for target assembly MF01: individual parts layout ( <i>top</i> ) and assembly of centering thimbles and sub-capsules ( <i>bottom</i> ). ....	14
Figure 14. Radiograph of targets MF01 and MF02. ....	15
Figure 15. Parts layout for the basket assembly. ....	15
Figure 16. Insertion of a capsule in the basket assembly ( <i>left</i> ), and top-down view of the basket after loading all targets ( <i>right</i> ). ....	16



## **TABLES**

Table 1. Materials and property references for thermal analyses. ....	5
Table 2. Test matrix for first mini fuel irradiation experiment. ....	6
Table 3. Peak midplane heat generation rates at beginning of cycle (BOC) and end of cycle (EOC).....	8



## ACRONYMS

AFC	Advanced Fuels Campaign
DOE-NE	Department of Energy, Office of Nuclear Energy
EABD	Experiment authorization basis document
HFIR	High Flux Isotope Reactor
HGR	Heat generation rate
LWR	Light water reactor
ORNL	Oak Ridge National Laboratory
PIE	Post-irradiation examination
PWR	Pressurized water reactor
QA	Quality assurance
SiC	Silicon carbide
TRISO	Tri-structural isotropic
UN	Uranium nitride
VXF	Vertical experiment facility

## **ACKNOWLEDGMENTS**

This work was supported by the US Department of Energy Office of Nuclear Energy (DOE-NE) Advanced Fuels Campaign (AFC). Neutron irradiation in the High Flux Isotope Reactor (HFIR) is made possible by the Office of Basic Energy Sciences, US DOE. The report was authored by UT-Battelle under Contract No. DE-AC05-00OR22725 with the US DOE. Alicia Raftery and David Bryant performed most of the capsule assembly work. Joel McDuffee and Josh Peterson-Droogh performed reviews of the thermal and neutronic calculations that support this work.

## **1. OBJECTIVE**

The objective of this work is to initiate the first series of miniature fuel specimen irradiations in the High Flux Isotope Reactor (HFIR) to facilitate rapid and cost-effective irradiation of novel fuel concepts. This first experiment will provide basic data on the irradiation performance of uranium nitride (UN) fuel kernels at relevant light water reactor temperatures.

## **2. INTRODUCTION**

Qualification of new nuclear fuel materials requires a scientific understanding of fuel behavior including irradiation performance. Traditionally, irradiation performance data has been acquired through many integral fuel irradiation experiments where full-size fuel pellets are tested under conditions that closely match those of the intended application. While this approach is logical, it is very expensive and time consuming, particularly when considering a large test matrix that could include variations in fuel centerline temperature, burnup, and power history or variations in the fuel itself such as composition, enrichment, grain size, impurities, or non-stoichiometries. Furthermore, the large number of variables that affect fuel performance make it difficult to develop fundamental models of various phenomena from integral fuel tests, which often have many independent variables that cannot be well-controlled. Therefore, there exists a need to be able to perform well-controlled separate effects irradiation testing of a wide range of new fuel concepts within a reasonable time and cost. Ideally these tests would be accelerated to accumulate burnup quickly. In addition, the testing platform should be flexible so that a range of fuel composition, enrichment, and even geometry can be tested without requiring detailed designs and analyses that are specific to each fuel concept.

This work reports on the successful implementation of a new capability for performing accelerated separate effects irradiation testing of miniature (“mini”) fuel specimens in the HFIR at Oak Ridge National Laboratory (ORNL). The design concept places the mini fuel specimens inside individually sealed sub-capsules inside steel targets in the reflector of the reactor. Temperature is controlled by sizing an insulating gas gap between the sub-capsules and the target housing. Reducing the size of the fuel allows for very high fission rates (on a per unit mass basis) without prohibitively large temperature gradients. Furthermore, the small fuel mass results in the total heat generated in each sub-capsule being dominated by gamma heating in the structure instead of fission in the fuel itself. This essentially decouples the fuel temperature from the fission rate. This work describes the design concept, neutronic and thermal analyses, and the fabrication, assembly, and delivery of the first set of experiments tested in the HFIR.

### 3. EXPERIMENT ANALYSIS METHODOLOGY

#### 3.1 Experiment design concept

Three-dimensional (3D) models of the experiment facility and an irradiation target are shown in Figure 1. The irradiation facility can accommodate as many as nine irradiation targets that are cooled at their outer surface by the reactor primary coolant. The irradiation facility is oriented so that the notch in the basket is pointed toward the reactor core. This allows for two of the three radial positions (positions 2 and 3) to be positioned at the same radial distance from the reactor core. These positions are expected to receive essentially the same neutron flux and gamma heating. Radial position 1 faces away from the core. Three targets are stacked vertically in each of the three radial target positions. Axial target positions 1, 2, and 3 correspond to the bottom, middle, and top positions, respectively. Each target contains six sealed titanium sub-capsules, each of which contains either four bare fuel kernels or six TRISO particles inside a molybdenum cup. Thimbles on either end of the sub-capsules insure centering of the sub-capsules within the target housing. Compression springs at both ends of the target housing keep the stacked parts in good contact. The sub-capsules each contain fuel specimens and SiC passive thermometry. The fuel specimens are surrounded by the molybdenum cup and tube to prevent chemical interaction with the titanium sub-capsule. A small hole in the sub-capsule end cap is used to perform the final seal weld of the sub-capsule. Temperature is controlled by varying the composition and size of the gas gap between the sub-capsule and the target housing. This gap depends primarily on gamma heating in the sub-capsule assembly components. The SiC thermometer is used to evaluate the irradiation temperature post-irradiation using dilatometry [1]. Experiments are irradiated in inner small vertical experiment facilities in the HFIR reflector. This first set of experiments were designed for an irradiation temperature of 500°C.

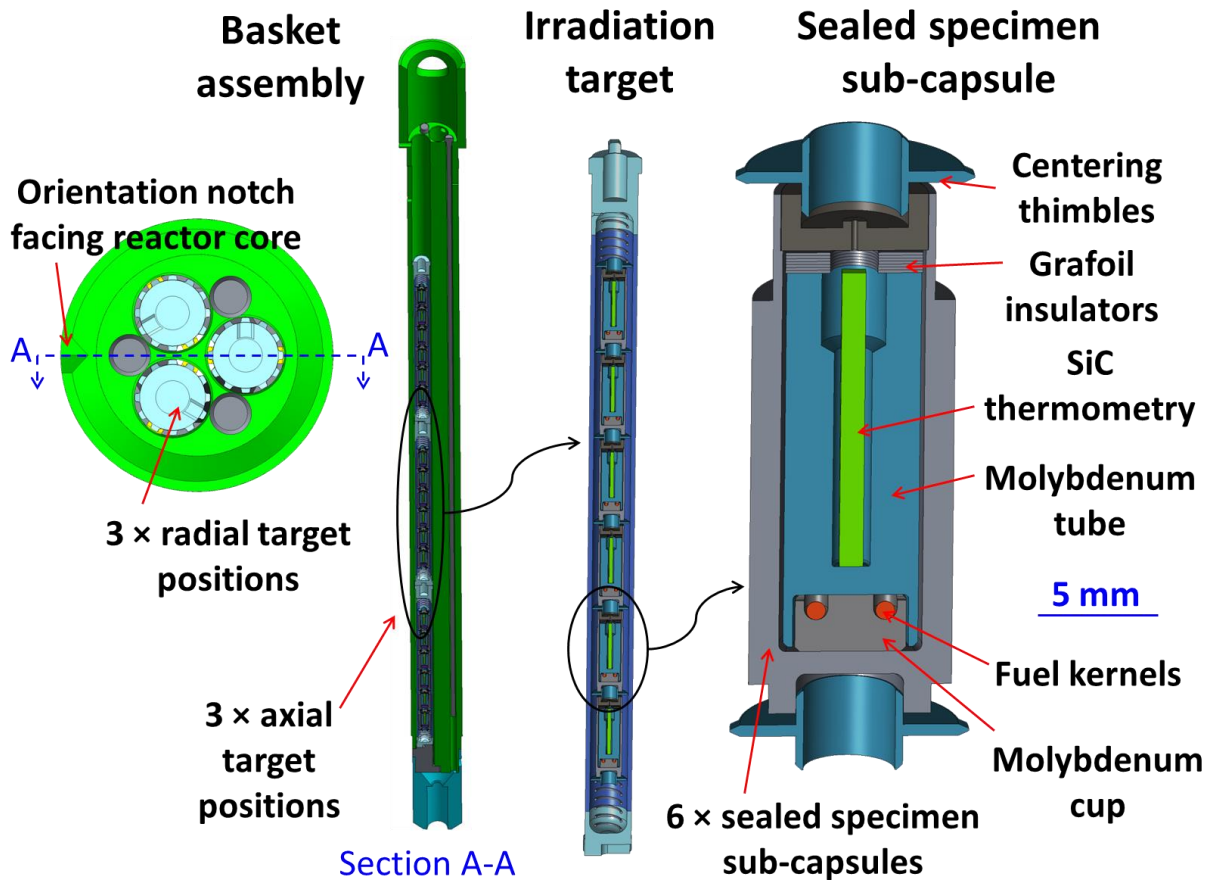


Figure 1. Irradiation design concept.

### 3.2 Neutronics analysis

Neutronics calculations are carried out to assess neutron and gamma heating rates in the fuel and capsule components to provide input to subsequent thermal analyses, as well as to generate initial fuel irradiation behavior predictions in terms of the fuel burnup profile. This is accomplished using the MCNP5 and SCALE software code packages. The MCNP calculations are based on existing beginning and end of cycle models [2] of the HFIR with cycle 400 experimental loading with some modifications to represent the new experimental assembly. The heat generation evaluation must account for contributions from fission neutrons (prompt and delayed), prompt fission photons, delayed photons from fission product decay,  $\alpha$  and  $\beta$  decay heat, and photon heating from local activation product decay. Prompt fission neutron and photon heating is calculated directly from MCNP transport simulations using an established fission neutron source distribution definition (with both neutron and photon tracking activated to implicitly yield an appropriate fission photon source distribution) [3]. Heat generation from these sources is then tallied in all experiment components. To account for heat generation from fission product decay photons originating in the HFIR fuel, a separate calculation is performed with a fixed photon source distribution definition reflecting the gamma emission rate and spectrum due to these accumulated fission products [3]. Activation and decay calculations are carried out using the ORIGEN module of the SCALE code package. Problem-

specific ORIGEN cross section data are generated with the COUPLE cross section processing module using 238-group neutron flux tallies from MCNP, enabling extended irradiation calculations with ORIGEN. These calculations yield local alpha and beta decay heating from activation products, as well as activation product gamma emission rates and spectra. This latter information is used to construct a local activation gamma source distribution definition for a final MCNP calculation assessing heat generation in the experimental capsule components from this photon source.

This methodology is implemented as described above for a thorough assessment of heat generation, burnup accumulation, and fission gas production for the first cycle of irradiation. These procedures may be extended with some modifications to assess later cycles of irradiation as well. Specifically, a Python script is employed to automate the coupling of flux magnitude and spectral results from MCNP to ORIGEN for depletion and decay assessment, followed by updating the MCNP models using the isotopics determined from ORIGEN [3]. In this manner, the irradiation experiment may be simulated for multiple cycles (currently up to 30); however, challenges remain with respect to reconciling the necessary computational time and rigor with the statistical reliability of the results. Efforts are underway to ameliorate these uncertainties by simplifying the temporal structure of the transport-depletion coupling sequence, generating reliable fixed representative cross section data, and by comparison against the SHIFT stochastic transport code. However, regardless of the precision of long-term burnup predictions, scoping studies have indicated that for fuel with the maximum allowable  $^{235}\text{U}$  enrichment (2.5 wt%), fuel heat generation decreases monotonically with increasing burnup. Therefore, fuel heat generation rates at the beginning of the first irradiation cycle are sufficient to bound the thermal design of the experimental assembly.

### 3.3 Thermal analysis

Thermal finite element calculations are performed using the ANSYS software code package with custom macros for determining thermal contact conductance between components and heat transfer through small movable (due to thermal expansion) gas gaps [4]. Figure 2 shows the CAD model for a single irradiation target and the resulting mesh after importing into ANSYS and applying  $\frac{1}{4}$ -symmetry. Minor components such as the target end caps, compression springs, fillets, and welds were removed. The remaining features were meshed with 20-node 3-D thermal solid elements with a nominal mesh size of 0.4 mm.

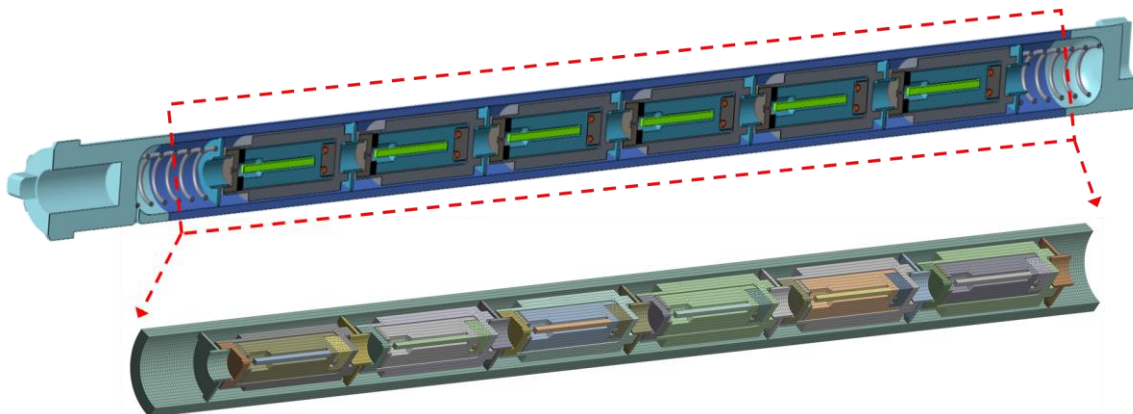


Figure 2. 3-D solid model for a single irradiation target and the resulting finite element mesh with  $\frac{1}{4}$ -symmetry.



Internal heat generation is applied to all components using the heat generation rates calculated in section 4.1. A convection boundary condition is applied to the outer surface of the target housing. Values of  $44.8 \text{ kW m}^{-2} \text{ K}^{-1}$  and  $58^\circ\text{C}$  were used for the convection heat transfer coefficient and bulk coolant temperature, respectively. These numbers were determined using RELAP5 for a previous fueled VXF irradiation experiment using the same facility. While the effects of fuel swelling and fission gas release are not considered in the thermal analyses, these effects are not expected to be significant since the fuel specimens are small ( $\sim 0.3 \text{ mm}^3$ ), and heat is primarily transferred via conduction from the bottom of the fuel specimens to the cup and then through the sub-capsules. The effects of thermal expansion are considered in the thermal contact conductance. The sub-capsule outer diameters and the fill gas can be varied to achieve the desired fuel temperatures.

Temperature-dependent material properties are used for all materials. Dose (or burnup)-dependent properties are used for SiC and UN. Some properties of the fuels also include porosity dependence. Table 1 summarizes the materials that are included in the thermal model and the references used for the material properties.

Table 1. Materials and property references for thermal analyses.

Material	Components	Property references
Titanium	Sub-capsules, centering thimbles	[5-7]
Silicon carbide	Thermometry	[6, 8]
304 stainless steel	Target housings	[6, 9]
Molybdenum	Tubes, cups	[6, 7]
UN	Fuel kernels	[10-15]
Grafoil	Insulators	[16]

### 3.4 Initial Test Matrix

This first mini fuel experiment will test UN fuel in the form of bare kernels and TRISO particles. Images of UN kernels and a UN TRISO particle are shown in Figure 3. The test matrix is summarized in Table 2. All fuel uses either natural or depleted uranium. For the kernels, several different carbon impurity levels and kernels densities are included. Some kernels include burnable absorbers (Gd) with varying absorber content. More details regarding the fuel fabrication can be found in previous work [17, 18].

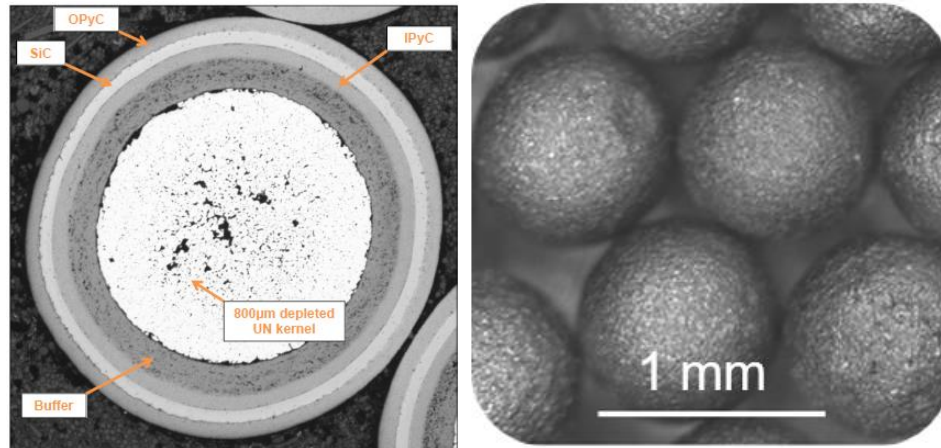


Figure 3. Polished cross-sectional image of UN TRISO particle (*left*) and image of UN kernels (*right*).

Table 2. Test matrix for first mini fuel irradiation experiment.

Fuel form	Kernel theoretical density	<sup>235</sup> U Enrichment (wt %)	Target burnup (% FIMA)
UC <sub>0.20</sub> N <sub>0.80</sub> kernels	94.9%	0.22%	1%, 6%
UC <sub>0.15</sub> N <sub>0.85</sub> kernels	90.6%	0.71%	
UC <sub>0.20</sub> N <sub>0.80</sub> kernels	90.9%	0.22%	
U <sub>0.89</sub> Gd <sub>0.11</sub> C <sub>0.11</sub> N <sub>0.89</sub> kernels	92.0%	0.71%	
U <sub>0.98</sub> Gd <sub>0.02</sub> C <sub>0.15</sub> N <sub>0.85</sub> kernels	93.6%	0.71%	
UC <sub>0.20</sub> N <sub>0.80</sub> TRISO particles	87.2%	0.22%	

## 4. EXPERIMENT ANALYSIS RESULTS

### 4.1 Neutronics analysis results

Figure 4 and Figure 5 show predicted heat generation rates (HGRs) in the titanium components and the molybdenum tubes as a function of distance from the core midplane ( $z$ ). Results are shown for the two radial target positions that face toward the HFIR core. Results are shown at beginning of cycle (BOC) and end of cycle (EOC) along with an exponential fit to each data set. Table 3 summarizes peak heating rates at the axial midplane of the core (the center axial target position) for all materials at BOC and EOC. Structural heat generation rates increase by 10–15% from BOC to EOC.

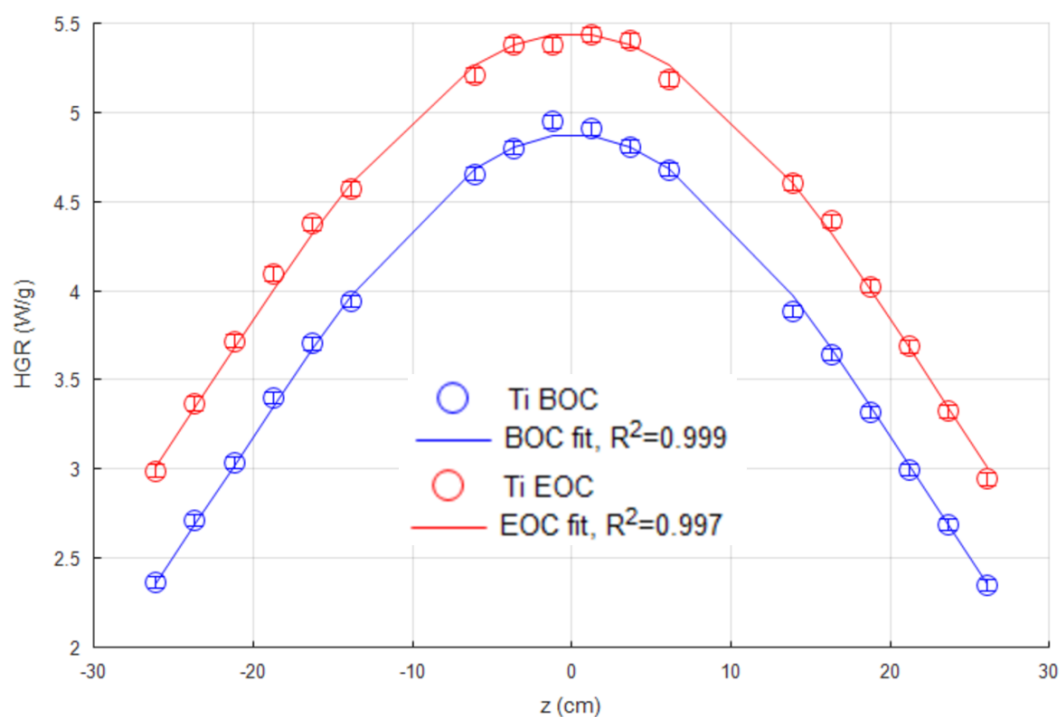


Figure 4. Heat generation rate (HGR) in titanium components vs. axial distance from the core midplane (z) at beginning of cycle (BOC) and end of cycle (EOC). Exponential fits to the calculated data are shown with goodness of fit parameter  $R^2$ .

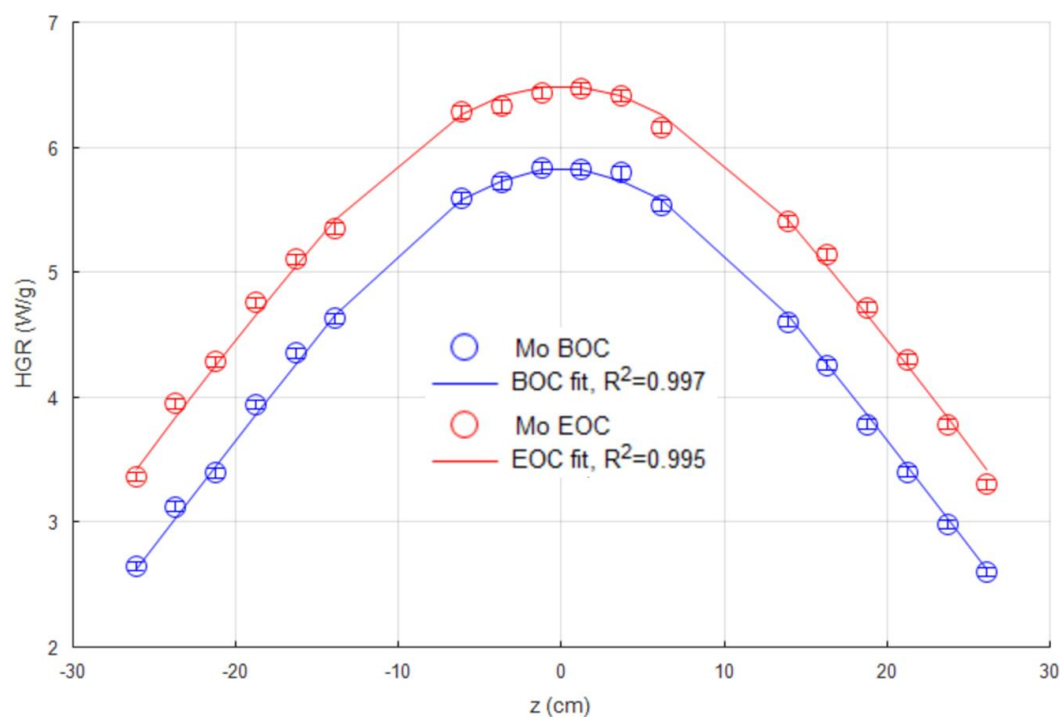


Figure 5. Heat generation rate (HGR) in the molybdenum tubes vs. axial distance from the core midplane (z) at beginning of cycle (BOC) and end of cycle (EOC). Exponential fits to the calculated data are shown with goodness of fit parameter  $R^2$ .

Table 3. Peak midplane heat generation rates at beginning of cycle (BOC) and end of cycle (EOC).

Component	Peak heat generation (W/g)	
	BOC	EOC
UN fuel with 0.22% $^{235}\text{U}$	$156.3 \pm 0.5^1$	
Stainless steel target	$4.52 \pm 0.10$	$4.92 \pm 0.12$
Titanium sub-capsules and centering thimbles	$4.87 \pm 0.18$	$5.44 \pm 0.22$
Molybdenum cup	$5.83 \pm 0.53$	$6.49 \pm 0.60$
Molybdenum tube	$6.07 \pm 0.29$	$6.75 \pm 0.34$
Silicon carbide thermometry	$3.98 \pm 0.28$	$4.35 \pm 0.31$
Grafoil	$3.99 \pm 0.37$	$4.38 \pm 0.42$
<sup>1</sup> Maximum heat generation rate over all cycles. Figure 6 shows how the fuel heating rate varies over time.		

The fuel heating rate changes significantly over time due to burnup of the initial  $^{235}\text{U}$  and breeding of fissile Pu isotopes. Figure 6 shows UN fuel fission heating rates and accumulated burnup (in percent fission of initial metal atoms, or FIMA) vs. the number of HFIR cycles for depleted uranium (0.22%  $^{235}\text{U}$ ), natural uranium (0.73%  $^{235}\text{U}$ ), and low-enriched uranium (2.5%  $^{235}\text{U}$ ). The calculated fuel heating rates and burnup use spatially-dependent total neutron flux and effective 1-group cross sections calculated from a highly rigorous MCNP run at the midpoint of the first irradiation cycle. This approach minimizes statistical uncertainties in the inputs to the depletion analysis, which assumes that the total neutron flux and the neutron flux energy spectra do not change significantly from cycle to cycle. This assumption seems reasonable given the small size of the fuel, which limits the impact of fuel transmutation on the neutron flux energy spectrum. Fuel heating rates do not change significantly after 5–7 cycles when an equilibrium is reached between breeding and burning of Pu isotopes and the majority of the  $^{235}\text{U}$  has been burned. Based on these results, it is anticipated that LWR discharge burnups of 6% FIMA can be achieved within 16 irradiation cycles, and that lesser burnups of 1% FIMA can be achieved within 4 cycles for fuel with depleted uranium. These predictions are to be compared against explicit long-term depletion calculations using the SHIFT code.

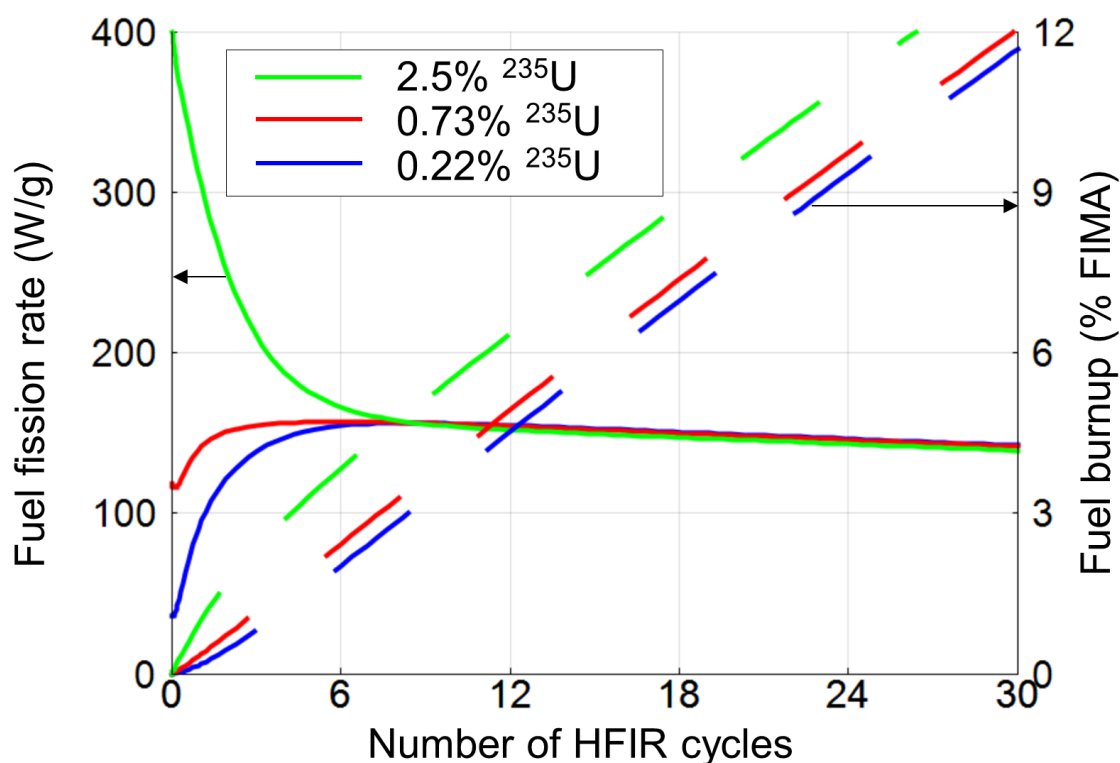


Figure 6. Calculated fuel fission rate (solid lines) and burnup (dashed lines) vs. number of HFIR cycles for three different enrichment levels. Results are for fuel located at the core midplane in radial targets oriented toward the HFIR core.

## 4.2 Thermal analysis results

Figure 7 shows temperature contours for a target containing UN fuel kernels with depleted uranium. These temperatures were calculated using EOC structural HGRs and peak fuel heating rates. The fill gas is a 40.5% He, Ar balance mixture. Despite the accelerated nature of the testing (i.e., high fuel fission rates), the temperature gradients in the fuel are relatively low (22°C) because of the small fuel size. The passive SiC temperature monitors have an average temperature of approximately 480°C (~70°C lower than the fuel temperatures) with temperature gradients of only 4°C. The passive SiC temperature monitors will be used to confirm the irradiation temperatures.

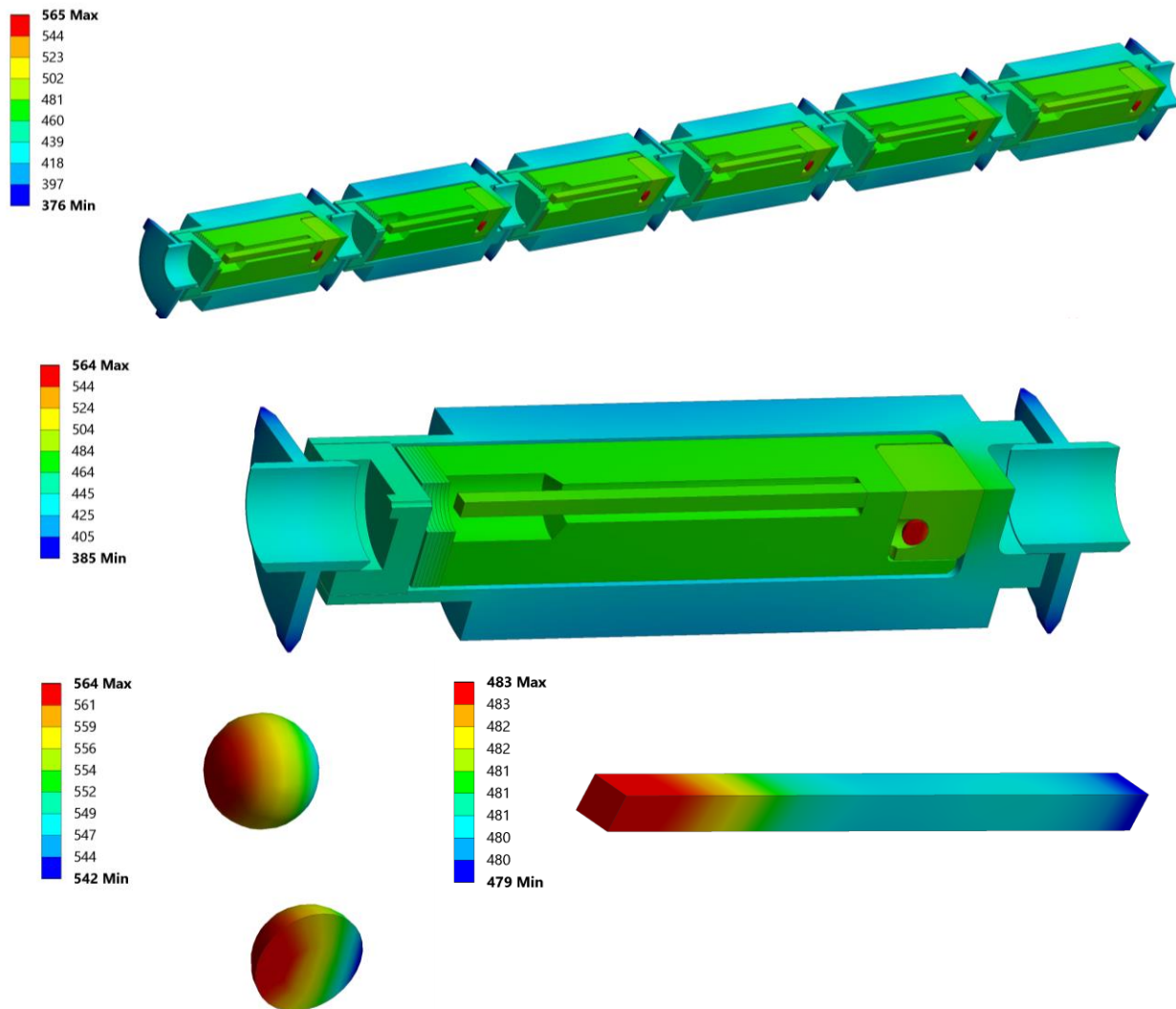


Figure 7. EOC temperature contours (in °C) with peak fuel heating rates for a target loaded in an inner radial position with six UN sub-capsules. Results show all target components (*top*), a single center sub-assembly (*middle*), the fuel kernels from the center sub-assembly (*bottom left*), and the temperature monitor from the center sub-assembly (*bottom right*).

Because the target temperature for all fuel specimens is approximately 500°C and there exist significant spatial gradients in the HGRs, the sub-capsule-to-housing gas gaps are adjusted to keep all fuel temperatures approximately the same. Figure 8 shows the design gas gaps vs. axial position for both inner radial target positions and outer radial target positions. Figure 9 and Figure 10 show the calculated temperatures for all fuel specimens at BOC with the minimum expected fuel fission rate and at EOC with peak fuel fission rates. The error bars in these figures indicate the maximum and minimum temperatures of the fuel at each location. The BOC and EOC cases that were evaluated cover the entire range of fuel temperatures that are expected during the experiment. All fuel temperatures remain within 75°C of the 500°C design temperature with most fuel temperatures remaining within 50°C.

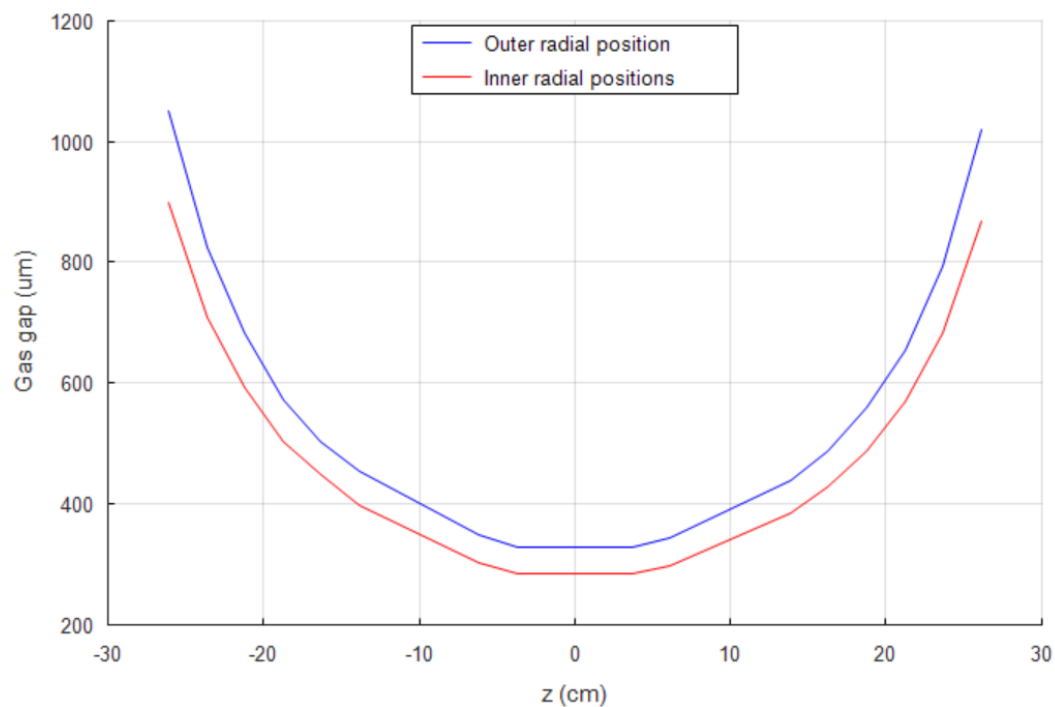


Figure 8. Design gas gaps between the sub-capsules and the target housing vs. axial distance from the core midplane for inner radial target positions and outer radial target positions.

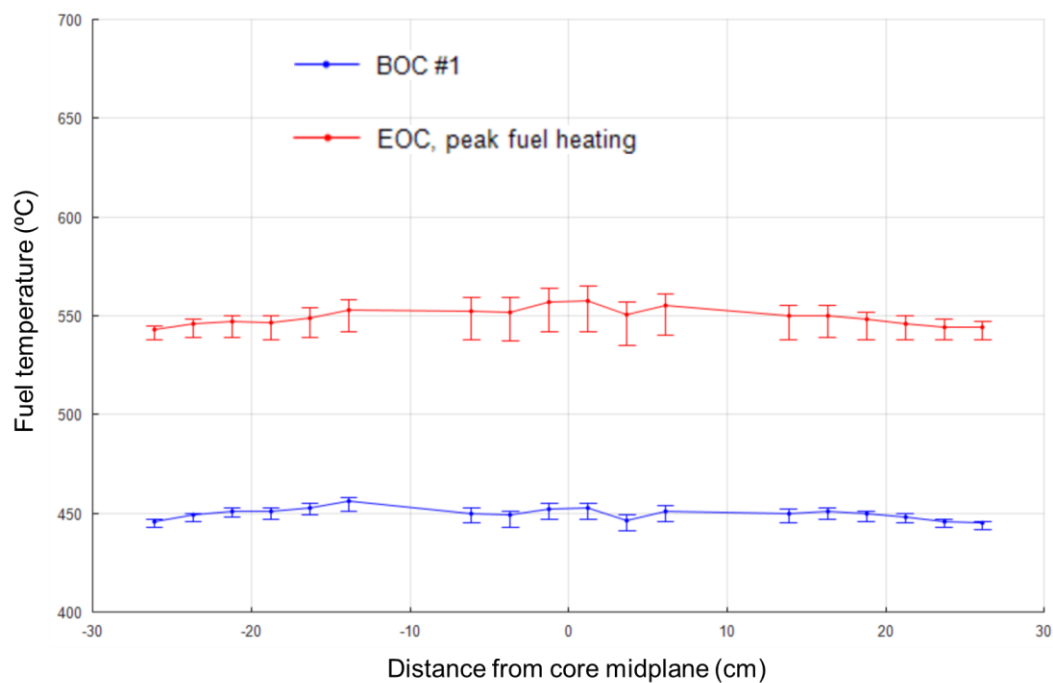


Figure 9. Fuel temperature vs. distance from the core midplane ( $z$ ) for an inner radial target position at beginning of cycle (BOC) and end of cycle (EOC). Error bars indicate the extreme fuel temperatures at each location.

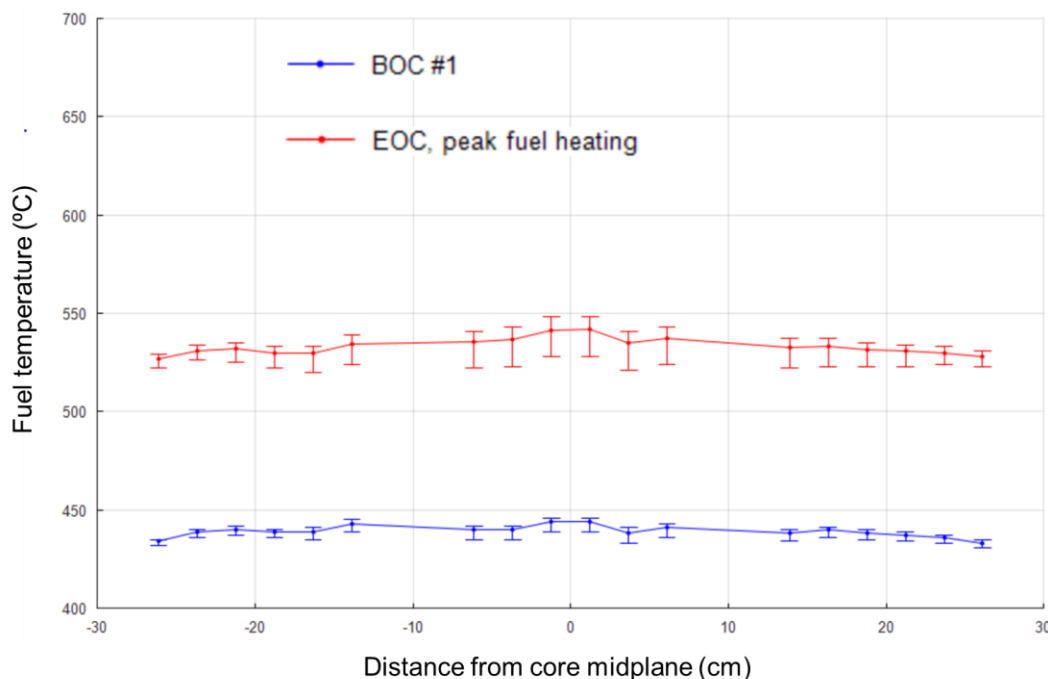


Figure 10. Fuel temperature vs. distance from the core midplane (z) for an outer radial target position at beginning of cycle (BOC) and end of cycle (EOC). Error bars indicate the extreme fuel temperatures at each location.

## 5. EXPERIMENT FABRICATION

### 5.1 Sub-capsules Assembly

A total of 12 sub-capsules were assembled. The parts layout for one sub-capsule is shown in Figure 11. The top image in the figure shows, from left to right, the cup (located inside a handling device that is not part of the assembly), the sub-capsule, the tube, the end cap, the thermometry, and the insulator disks. The bottom left image shows 6 UN kernels loaded inside one fuel cup. The bottom right image shows 4 UN TRISO particles loaded inside a different fuel cup.

Once the fuel specimens were placed in the cup, the sub-capsule was loaded with the cup and the molybdenum tube containing the thermometry. Figure 12 shows a top view of a loaded sub-capsule: insulator disks are placed above the tube and the thermometry is visible at the center of the sub-capsule. The signed sub-assembly fabrication request forms are provided in Appendix A.





Figure 11. Sub-capsule part layout (*top*), kernel fuel inside a cup (*bottom left*), and TRISO particle fuel inside a different cup (*bottom right*).

All sub-capsule components were dimensionally inspected and cleaned according to HFIR-approved procedures, drawings, and sketches. After assembly of the internal components, all sub-capsule end caps were welded to the sub-capsule bodies using an electron beam weld. The sub-capsule assemblies were then placed inside sealed containers that were evacuated and backfilled with ultra-high-purity helium three times to ensure a pure environment. The containers were placed inside a glove box, which was also evacuated and backfilled with the same gas used in the sealed containers. Each sub-capsule end cap has a small hole that was seal-welded using a gas tungsten arc welding procedure. All welds passed visual examination. Each sub-capsule was then sent for nondestructive examination, which included a bubble test and a helium leak test. All assemblies passed the nondestructive examination.



Figure 12. Top view of a loaded sub-capsule without its end cap (*left*) and welded sub-capsules (*right*).

## 5.2 Target Assembly

A total of 2 targets, each containing 6 sub-capsules were assembled. The parts layout for one target assembly is shown in Figure 13. As shown in this figure, the target bottom end cap was welded to the target housing prior to loading the sub-capsules. The signed capsule fabrication request forms are provided in Appendix A.



Figure 13. Parts layout for target assembly MF01: individual parts layout (*top*) and assembly of centering thimbles and sub-capsules (*bottom*).

All target components were dimensionally inspected and cleaned according to HFIR-approved procedures, drawings, and sketches. After loading the sub-capsules, centering thimbles, and compression springs, the target top end caps were orbital welded to the target housing. The targets were then placed inside a sealed container that was evacuated and backfilled with an ultra-high-purity helium/argon gas mixture three times to ensure a pure environment. The containers were placed inside a glove box, which was also evacuated and backfilled with the same gas used in the sealed container. Each target assembly

has a small hole in the top end cap that was seal-welded using a gas tungsten arc welding procedure. All welds passed visual examination. Each target assembly was then sent for nondestructive examination, which included a helium leak test, hydrostatic compression at a pressure of 1,035 psi, mass comparisons before and after hydrostatic compression to ensure no water penetrated the target assembly, another post-compression helium leak test, dye penetrant inspection, and radiographic inspection (see Figure 14). All target assemblies passed the nondestructive examination.

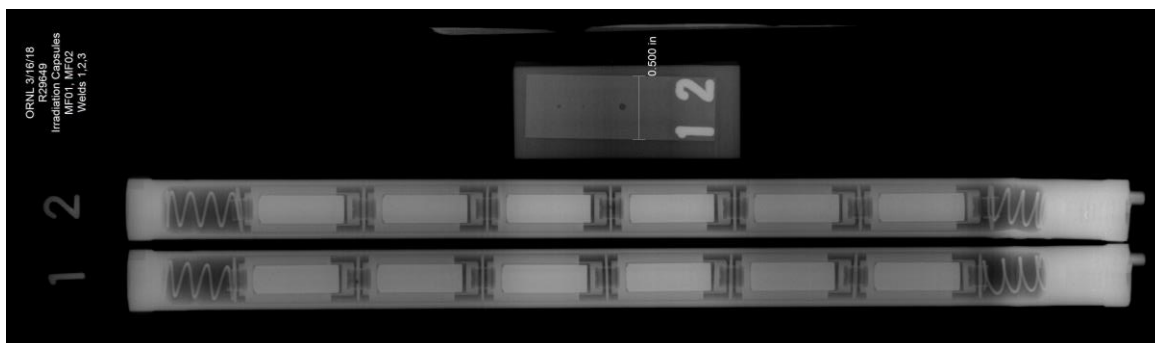


Figure 14. Radiograph of targets MF01 and MF02.

### 5.3 Basket Assembly

The irradiation targets must be loaded into a basket assembly to keep the targets centered within the flow channel in the HFIR small vertical experiment facility. A total of 9 targets were assembled inside the basket with the configuration shown in Figure 1. For this experiment, only two fueled targets (MF01 and MF02) were included. The remaining seven targets (D01 through D07) were stainless steel dummies. Figure 15 shows the parts layout for the basket assembly including the fueled targets, dummies, and the basket itself. Figure 16 shows the insertion of a target in the basket assembly as well as a top-down view of the basket prior after loading all targets. The signed assembly fabrication request form is provided in Appendix A.



Figure 15. Parts layout for the basket assembly.





Figure 16. Insertion of a capsule in the basket assembly (*left*), and top-down view of the basket after loading all targets (*right*).

## 5.4 Fabrication Package and Delivery to HFIR

Each irradiation experiment requires a fabrication package that is reviewed by an independent design engineer, a lead quality assurance (QA) representative, and a HFIR QA representative before acceptance for insertion into the HFIR. The fabrication package must satisfy the requirements of the experiment authorization basis document (EABD). The irradiation of miniature fuel specimens experiment falls under document EABD-HFIR-2018-001. This document specifies several requirements that the rabbits must satisfy in the areas of

- thermal safety analyses,
- material certification,
- dimensional inspection,
- cleaning,
- assembly procedure,
- sample loading,
- fill gas,
- welding, and
- nondestructive evaluation.

The fabrication package for the basket assembly MFA was reviewed and approved by all parties and accepted by HFIR on May 29, 2018. The final signed acceptance page of the EABD is provided in Appendix A. The basket assembly was inserted during HFIR cycle 480 (June 2018).

## 6. SUMMARY AND CONCLUSIONS

This report summarizes the design concept and the fabrication of the first series of miniature fuel irradiation experiments supported by the Advanced Fuels Campaign. This first experiment was successfully assembled and delivered to the HFIR for insertion during cycle 480 (June 2018). The experiment contains six different types of UN-based fuel kernels UN TRISO particles, which will be evaluated post-irradiation to determine swelling, fission gas release, and microstructural evolution. The sub-capsules, targets, and basket were successfully assembled, welded, evaluated, and delivered to the HFIR along with a complete QA fabrication package. Pictures of the assembly process are included in this report. Documentation of the experiment fabrication and final acceptance by the HFIR is provided in an appendix. The data that will be obtained from post-irradiation examination of the irradiated specimens will help support the evaluation of new fuel concepts for commercial applications to ultimately improve the accident tolerance and economics of LWRs.

## 7. REFERENCES

1. Campbell, A., et al., *Method for analyzing passive silicon carbide thermometry with a continuous dilatometer to determine irradiation temperature*. Nuclear Instruments and Methods in Physics Research B, 2016. **370**: p. 49–58.
2. Xoubi, N. and R.T. Primm Iii, *Modeling of the High Flux Isotope Reactor Cycle 400*, ORNL/TM-2004/251, Oak Ridge, TN (2005).
3. Chandler, D., *Activation and heat generation calculations to support Pu-238 fully loaded target irradiations in inner small VXF's for up to three cycles*, C-HFIR-2015-014, Oak Ridge National Laboratory: Oak Ridge, TN (2015).
4. McDuffee, J.L., *Heat Transfer Through Small Moveable Gas Gaps in a Multi-Body System Using the ANSYS Finite Element Software*, in *Proceedings of ASME 2013 Heat Transfer Summer Conference*. 2013: Minneapolis, MN, United States. p. 17783.
5. M. Boivineau, C.C., D. Doytier, V. Eyraud, M.-H. Nadal, B. Wilthan, G. Pottlacher, *Thermophysical Properties of Solid and Liquid Ti-6Al-4V (TA6V) Alloy*. International Journal of Thermophysics, 2006. **27**(507).
6. Cindas, L. *Global Benchmark for Critically Evaluated Materials Properties Data*. [cited 2016 July, 27]; Available from: <http://cindasdata.com>.
7. Matweb. *Material Property Data*. [cited 2016 July 27]; Available from: <http://matweb.com/>.
8. L. L. Snead, T.N., Y. Katoh, T.-S. Byun, S. Kondo, D. A. Petti, *Handbook of SiC properties for fuel performance modeling*. Journal of Nuclear Materials, 2007. **371**(329).
9. Asme, *Boiler and Pressure Vessel Code*, in *Section II - Materials (Includes Addenda for 2011)*. 2010, American Society of Mechanical Engineers.
10. S. L. Hayes, J.K.T., K. L. Peddicord, *Material property correlations for uranium mononitride: I. Physical properties*. Journal of Nuclear Materials, 1990. **171**.
11. S. L. Hayes, J.K.T., K. L. Peddicord, *Material property correlations for uranium mononitride: II. Mechanical properties*. Journal of Nuclear Materials, 1990. **171**.
12. S. L. Hayes, J.K.T., K. L. Peddicord, *Material property correlations for uranium mononitride: IV. Thermodynamic properties*. Journal of Nuclear Materials, 1990. **171**.
13. Collin, B., *Modeling and Analysis of FCM UN TRISO Fuel Using the PARFUME Code*, Idaho National Laboratory: Idaho Falls, ID (2013).
14. S. B. Ross, M.S.E.-G., R. B. Matthews, *Thermal conductivity correlation for uranium nitride fuel between 10 and 1923 K*. Journal of Nuclear Materials, 1988. **151**.

15. U. C. Nunez, D.P., R. Bohler, D. Manara, *Melting point determination of uranium nitride and uranium plutonium nitride: A laser heating study*. Journal of Nuclear Materials, 2014. **449**.
16. *Grafoil Engineering Manual*. 2002; 2nd Edition:[Available from: <http://www.graftech.com/wp-content/uploads/2014/12/GRAFOIL-Engineering-Manual-2nd-Ed.pdf>].
17. McMurray, J.W., et al., *Production of Low-Enriched Uranium Nitride Kernels for TRISO Particle Irradiation Testing*, ORNL/SR-2016/268, Oak Ridge National Laboratory: Oak Ridge, TN (2016).
18. Jolly, B., et al., *Fabrication and Characterization of DU and LEU UN TRISO Particles*, ORNL/LTR-2016/384, Oak Ridge National Laboratory: Oak Ridge, TN (2016).

## **APPENDIX A. FABRICATION AND QUALITY ASSURANCE DOCUMENTATION FOR EXPERIMENTS**

Basket ID: MFA

Irradiation Conditions  
 Small VXF Position VXF-15  
 Initial cycle 479  
 Assembly Drawing X3E020977A725, Rev. 1

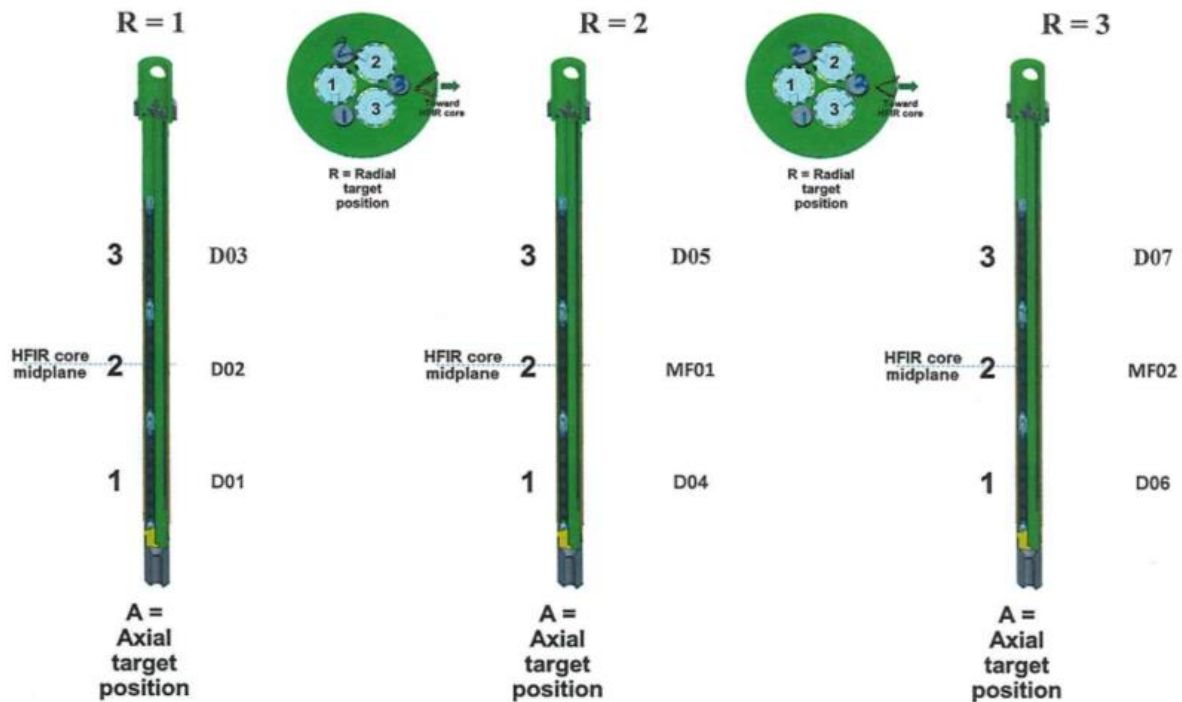
## Approvals

	Request	Build
Performed by:	Chris Petrie 3/27/18	3/26/18
Checked by:	3/27/18	3/26/18

## Basket Loading

Component	Drawing	Rev.	Part	Material	Count	Comment	MAT IR	FAB IR	ID	Mass (g)
Basket center section	X3E020977A729	2	1	Al 6061	1		18193*	20814	MFA	1612.60
Orifice	X3E020977A674	1	1	Al 6061	1		20816*	20816	18-01	175.66
Support web	X3E020977A729	2	2	304 SS	1		19575*	20815	18-01	35.61
Dummy flux monitor	X3E020977A722	2	5	Al 6061	3		19348	20819	01	15.69
						02			15.68	
						03			15.69	
Dummy capsule	X3E020977A722	2	4	304 SS	1	R-A = 1-1	20813*	20813	D01	186.46
Dummy capsule			4	304 SS	1	R-A = 1-2	20813	20813	D02	186.40
Dummy capsule			4	304 SS	1	R-A = 1-3	20813	20813	D03	186.66
Dummy capsule			4	304 SS	1	R-A = 2-1	20813	20813	D04	186.17
Experiment capsule assembly			1	N/A	1	R-A = 2-2	N/A	20820	MF01	125.98
Dummy capsule			4	304 SS	1	R-A = 2-3	20813	20813	D05	186.68
Dummy capsule			4	304 SS	1	R-A = 3-1	20813	20813	D06	186.73
Experiment capsule assembly			1	N/A	1	R-A = 3-2	N/A	20820	MF02	126.06
Dummy capsule			4	304 SS	1	R-A = 3-3	20813	20813	D07	186.21

Capsule	R = Radial position	A = Axial position	Number cycles	Dummy?	Fill gas	1st cycle	Temperature (°C)
D01	1	1	16	YES	N/A	479	600
D02	1	2	16	YES	N/A	479	600
D03	1	3	16	YES	N/A	479	600
D04	2	1	16	YES	N/A	479	600
MF01	2	2	3	NO	40.5% He, Ar bal	479	600
D05	2	3	16	YES	N/A	479	600
D06	3	1	16	YES	N/A	479	600
MF02	3	2	16	NO	40.5% He, Ar bal	479	600
D07	3	3	16	YES	N/A	479	600





# Capsule Fabrication Request Sheet

P of 1  
Date 3/15/18

Target ID: MF01  
Irradiation Conditions  
Irradiation Location (R, A) 2 2  
Number cycles 3  
First Cycle Goal 479  
Fill Gas 40.5% He, Ar bal  
Irradiation Temperature 600°C  
Assembly drawing X3E020977A722, Rev. 2

## Approvals

	Request	Build
Performed by:	Chris Peltier 3/15/18	3/14/18
Checked by:	NSE 3-15-18	Shawn M. Koffey 3/15/18

## Capsule Fabrication

Component	Drawing	Rev.	Part	Material	Count	Comment	MAT IR	FAB IR	ID	Mass (g)
Capsule outer tube	X3E020977A520	A	2	304 SS	1		20789 *	20789	17-01	54.1860
Capsule bottom end cap	X3E020977A520	A	3	304 SS	1		20790 *	20790	17-01	8.3650
Capsule top end cap	X3E020977A520	A	4	304 SS	1		20791 *	20791	17-01	16.0540
Spring	X3E020977A722	2	3	304 SS	2		20810	20810	1	0.2610
									2	0.2620
Centering thimble	X3E020977A722	2	2	Ti-6Al4V	7		20803	20803	18-01	0.1746
									18-02	0.1708
									18-03	0.1724
									18-04	0.1712
									18-05	0.1713
									18-06	0.1700
									18-07	0.1747
Holder assembly	S17-13-CER_FUEL	1	1	N/A	6	2-2-6	N/A	20821	H26-01	7.5900
						2-2-5			H27-01	7.6321
						2-2-4			H27-02	7.6217
						2-2-3			H27-03	7.6212
						2-2-2			H27-04	7.6335
						2-2-1			H25-01	7.5530
Total Mass										125.9845

## Holder Sub-Assemblies

Holder ID	S = Sub-Assembly Position	R-A-S (R = Radial target position, A = Axial target position)	Holder diameter (mm)	Initial
H26-01	6	2-2-6	9.46	DB
H27-01	5	2-2-5	9.49	DB
H27-02	4	2-2-4	9.49	DB
H27-03	3	2-2-3	9.49	DB
H27-04	2	2-2-2	9.49	DB
H25-01	1	2-2-1	9.45	DB

## Capsule Fabrication Request Sheet

Page 1 of 1  
Date 2018

Target ID: MF01

## Irradiation Conditions

Irradiation Location (R, A) 2 2  
 Number cycles 3  
 First Cycle Goal 479  
 Fill Gas 40.5% He, Ar bal  
 Irradiation Temperature 600°C  
 Holder assembly drawing S17-13-CER\_FUEL, Rev. 1

## Approvals

Request Build  
 Performed by: Chris Reber 3-9-18 Adam M. Raftoy 3-15-18  
 Checked by: [Signature] 3-13-18 [Signature] 3-19-18

## Holder Assembly

Component	Drawing	Rev.	Part	Material	MAT IR	FAB IR	S = 1	S = 2	S = 3	S = 4	S = 5	S = 6	S = 1	S = 2	S = 3	S = 4	S = 5	S = 6	All	
Holder	S17-14-CER_FUEL	1	1	Ti-6Al4V	20803	20804	H25-01	H27-04	H27-03	H27-02	H27-01	H26-01	3.5578	3.5876	3.6087	3.5992	3.599	3.5639	21.5159	
End cap	S17-14-CER_FUEL	1	2	Ti-6Al4V	20803	20805	18-01	18-02	18-03	18-04	18-05	18-06	0.2242	0.2246	0.2241	0.2230	0.223	0.2238	1.3429	
Tube	S17-13-CER_FUEL	1	2	Moly	20611	20806	18-01	18-02	18-03	18-04	18-05	18-06	3.3336	3.3509	3.3185	3.3398	3.358	3.3601	20.0604	
Thermometry	S17-13-CER_FUEL	1	3	SiC	19502	20802	1	2	3	4	5	13	0.0436	0.0436	0.043	0.0431	0.042	0.0434	0.2586	
Insulator disks (list total # and mass)	S17-13-CER_FUEL	1	4	Grafoil	19812	19812	5	5	5	5	5	5	0.012	0.012	0.012	0.012	0.012	0.012	0.072	
Disk fuel dish	S17-26-CER_FUEL	1	2	Moly	20611	20808	N/A	N/A	N/A	N/A	N/A	N/A	N/A	N/A	N/A	N/A	N/A	N/A	0	
Disk fuel specimen	S17-26-CER_FUEL	1	3	UO2	20818	20818	N/A	N/A	N/A	N/A	N/A	N/A	N/A	N/A	N/A	N/A	N/A	N/A	0	
Bare kernel fuel dish	S17-24-CER_FUEL	1	2	Moly	20611	20807	18-01	18-02	18-03	18-04	18-05	N/A	0.3977	0.3948	0.3993	0.3791	0.375	N/A	1.9459	
Bare kernel fuel specimen	S17-24-CER_FUEL	1	3	UN	20811	20811	A1	B1	C1	D1	E1	N/A	0.0038	0.0034	0.0023	0.0045	0.0040	N/A	0.018	
							A2	B2	C2	D2	E2	N/A	0.0036	0.0033	0.0029	0.0043	0.0040	N/A	0.0181	
							A3	B3	C3	D3	E3	N/A	0.0036	0.0032	0.0027	0.0041	0.0048	N/A	0.0184	
							A4	B4	C4	D4	E4	N/A	0.0032	0.0032	0.0028	0.0040	0.0042	N/A	0.0174	
							A5	B5	C5	D5	E5	N/A	0.0034	0.0028	0.0026	0.0040	0.0043	N/A	0.0171	
							A6	B6	C6	D6	E6	N/A	0.0035	0.0027	0.0028	0.0041	0.0039	N/A	0.017	
Coated particle fuel dish	S17-27-CER_FUEL	1	2	Moly	20611	20809	N/A	N/A	N/A	N/A	N/A	18-01	N/A	N/A	N/A	N/A	N/A	0.3272	0.3272	
Coated particle fuel specimen	S17-27-CER_FUEL	1	3	UN	20812	20812	N/A	N/A	N/A	N/A	N/A	F1	N/A	N/A	N/A	N/A	N/A	0.0060	0.006	
							N/A	N/A	N/A	N/A	N/A	F2	N/A	N/A	N/A	N/A	N/A	0.0058	0.0058	
							N/A	N/A	N/A	N/A	N/A	F3	N/A	N/A	N/A	N/A	N/A	0.0055	0.0055	
							N/A	N/A	N/A	N/A	N/A	F4	N/A	N/A	N/A	N/A	N/A	0.0053	0.0053	
Total Fuel							7.5900	7.6321	7.6217	7.6212	7.6335	7.5530	45.6515	0.0211	0.0186	0.0161	0.0250	0.0252	0.0226	0.1285

CME 4-12-18

Capsule Fabrication Request Sheet

P 1 of 1  
Date 3/15/18

Target ID: MF02  
Irradiation Conditions  
Irradiation Location (R, A) 3 2  
Number cycles 16  
First Cycle Goal 479  
Fill Gas 40.5% He, Ar bal  
Irradiation Temperature 600°C  
Assembly drawing X3E020977A722, Rev. 2

Approvals

Request	Build
Performed by: Chris Redick 3-15-18	3/14/18 [Signature]
Checked by: [Signature] 3-15-18	Heidi M. Kefauver 3/15/18

Capsule Fabrication

Component	Drawing	Rev.	Part	Material	Count	Comment	MAT IR	FAB IR	ID	Mass (g)
Capsule outer tube	X3E020977A520	A	2	304 SS	1		20789	20789	17-02	54.5260
Capsule bottom end cap	X3E020977A520	A	3	304 SS	1		20790	20790	17-02	8.3910
Capsule top end cap	X3E020977A520	A	4	304 SS	1		20791	20791	17-02	15.9490
Spring	X3E020977A722	2	3	304 SS	2		20810	20810	3	0.2580
									4	0.2640
Centering thimble	X3E020977A722	2	2	Ti-6Al4V	7		20803	20803	18-08	0.1718
									18-09	0.1648
									18-10	0.1736
									18-11	0.1708
									18-12	0.1650
									18-13	0.1677
									18-14	0.1727
Holder assembly	S17-13-CER_FUEL	1	1	N/A	6	3-2-6	N/A	20821	H26-02	7.5657
						3-2-5			H27-05	7.6064
						3-2-4			H27-06	7.6039
						3-2-3			H27-09	7.5982
						3-2-2			H27-08	7.5948
						3-2-1			H25-02	7.5202
Total Mass										126.0636

Holder Sub-Assemblies

Holder ID	S = Sub-Assembly Position	R-A-S (R = Radial target position, A = Axial target position)	Holder diameter (mm)	Initial
H26-02	6	3-2-6	9.46	DB
H27-05	5	3-2-5	9.49	DB
H27-06	4	3-2-4	9.49	DB
H27-09	3	3-2-3	9.49	DB
H27-08	2	3-2-2	9.49	DB
H25-02	1	3-2-1	9.45	DB

# Irradiation of Miniature Fuel Specimens in the High Flux Isotope Reactor

June 2018

A-6

## Capsule Fabrication Request Sheet

Page 1 of 1  
Date: 3/15/18

Target ID: MF02

**Irradiation Conditions**

Irradiation Location (R, A) 3 2

Number cycles 16

First Cycle Goal 479

Fill Gas 40.5% He, Ar bal

Irradiation Temperature 600°C

Holder assembly drawing S17-13-CER\_FUEL, Rev. 1

**Approvals**

Request	Build
Chris Lettice 3-9-18	Aluc M. Kaptey 3-15-18
3-13-18	3-19-18

Holder Assembly							Component IDs for each holder ID						Component mass (g) for each holder ID									
Component	Drawing	Rev.	Part	Material	MAT IR	FAB IR	S = 1	S = 2	S = 3	S = 4	S = 5	S = 6	S = 1	S = 2	S = 3	S = 4	S = 5	S = 6	All			
Holder	S17-14-CER_FUEL	1	1	TI-6Al4V	20803	20804	H25-02	H27-08	H27-09	H27-06	H27-05	H26-02	3.55	3.5932	3.5917	3.5954	3.591	3.5652	21.4867			
End cap	S17-14-CER_FUEL	1	2	TI-6Al4V	20803	20805	18-07	18-08	18-09	18-10	18-11	18-12	0.2239	0.2233	0.2242	0.2237	0.224	0.2243	1.3429			
Tube	S17-13-CER_FUEL	1	2	Moly	20611	20806	18-07	18-08	18-09	18-10	18-11	18-12	3.3363	3.3374	3.3377	3.3238	3.326	3.3271	19.988			
Thermometry	S17-13-CER_FUEL	1	3	SiC	19502	20802	7	8	9	10	11	12	0.0434	0.0428	0.0434	0.0428	0.043	0.0433	0.2589			
Insulator disks (list total # and mass)	S17-13-CER_FUEL	1	4	Grafoil	19812	19812	5	5	5	5	5	5	0.012	0.012	0.012	0.012	0.012	0.012	0.072			
Disk fuel dish	S17-26-CER_FUEL	1	2	Moly	20611	20808	N/A	N/A	N/A	N/A	N/A	N/A	N/A	N/A	N/A	N/A	N/A	N/A	0			
Disk fuel specimen	S17-26-CER_FUEL	1	3	UCO2	20818	20818	N/A	N/A	N/A	N/A	N/A	N/A	N/A	N/A	N/A	N/A	N/A	N/A	0			
Bare kernel fuel dish	S17-24-CER_FUEL	1	2	Moly	20611	20807	18-06	18-07	18-08	18-09	18-10	N/A	0.3793	0.3772	0.3758	0.3764	0.376	N/A	1.8844			
Bare kernel fuel specimen	S17-24-CER_FUEL	1	3	UN	20611	20811	A7	B7	C7	D7	E7	N/A	0.0035	0.0034	0.0029	0.0041	0.0040	N/A	0.0179			
							A8	B8	C8	D8	E8	N/A	0.0036	0.0035	0.0033	0.0042	0.0033	N/A	0.0179			
							A9	B9	C9	D9	E9	N/A	0.0033	0.0035	0.0034	0.0041	0.0038	N/A	0.0181			
							A10	B10	C10	D10	E10	N/A	0.0035	0.0032	0.0028	0.0039	0.0043	N/A	0.0177			
							A11	B11	C11	D11	E11	N/A	0.0038	0.0032	0.0037	0.0040	0.0042	N/A	0.0189			
							A12	B12	C12	D12	E12	N/A	0.0031	0.0037	0.003	0.0038	0.0039	N/A	0.0175			
Coated particle fuel dish	S17-27-CER_FUEL	1	2	Moly	20611	20809	N/A	N/A	N/A	N/A	N/A	18-02	N/A	N/A	N/A	N/A	N/A	0.3263	0.3263			
Coated particle fuel specimen	S17-27-CER_FUEL	1	3	UN	20812	20812	N/A	N/A	N/A	N/A	N/A	F5	N/A	N/A	N/A	N/A	N/A	0.0056	0.0056			
							N/A	N/A	N/A	N/A	N/A	F6	N/A	N/A	N/A	N/A	N/A	0.0054	0.0054			
							N/A	N/A	N/A	N/A	N/A	F7	N/A	N/A	N/A	N/A	N/A	0.0058	0.0058			
							N/A	N/A	N/A	N/A	N/A	F8	N/A	N/A	N/A	N/A	N/A	0.0052	0.0052			
Total Fuel												7.5657	7.6063	7.6039	7.5982	7.5948	7.5202	7.5992	45.4891			
												0.0208	0.0208	0.0191	0.0241	0.0235	0.0220	0.0200	0.1259			

CME 4-12-18

7.6063  
0.0204

45.4891  
0.1259

ALC  
3/27/2018

## Section 6: Acceptance for Use of As-Built Experiment Capsule

Note: This section is used to document acceptance of the as-built experiment for reactor installation and irradiation. This section is completed **after** completion of Section 2. See notes for explanation of signatures.

### 1. List Applicable Component Identifications:

Basket ID: MFA

Sub-capsule I.D.	Target I.D.
H25-01 (2-2-1)	MF01
H27-04 (2-2-2)	MF01
H27-03 (2-2-3)	MF01
H27-02 (2-2-4)	MF01
H27-01 (2-2-5)	MF01
H26-01 (2-2-6)	MF01
H25-02 (3-2-1)	MF02
H27-08 (3-2-2)	MF02
H27-09 (3-2-3)	MF02
H27-06 (3-2-4)	MF02
H27-05 (3-2-5)	MF02
H26-02 (3-2-6)	MF02

### 2. Approvals (see notes for explanation of signature responsibilities)

Christian Petric  
Lead Experimenter

Mark C. Vause  
Lead QA

L. C. Smith

RRD NQR

Greg Hirtz

E&FI Staff

N. O. Huff

RRD Criticality Safety Officer

FULLER, BRIANE ①  
HFIR MBA Representative

FULLER, BRIANE  
HFIR Operations (print name)

Chris Petric  
Lead Experimenter (signature)

Mark C. Vause  
Lead QA (signature)

L. C. Smith

RRD QA (signature)

Greg Hirtz  
E&FI Staff (signature)

N. O. Huff

RRD Criticality Safety Officer (signature)

Brian E Fuller  
HFIR MBA Representative (signature)

Brian E Fuller  
HFIR Operations (signature)

5-24-18  
Date

5/24/18  
Date

5/25/18

Date

5/29/18

Date

5/21/18  
Date

05/29/2018  
Date

05/24/2018  
Date

① NO NMCA REQUIREMENTS. BE7